FROZEN WAVE GENERATOR TECHNOLOGY AS A SOURCE OF CONSTANT AMPLITUDE HIGH POWER HIGH FREQUENCY RADIO FREQUENCY PULSES *

S. Best[ξ], M. F. Rose, Z. Shotts
Radiance Technologies, Inc., 1490 Pumphrey Ave
Auburn, Alabama, U.S.A.

M. Rader[Ψ], L. L. Altgilbers
U.S. Army Space and Missile Defense Command / Army Strategic Forces Command
Huntsville, Alabama, U.S.A.

Abstract

A Frozen Wave Generator as a source of RF energy consists of an ensemble of electrostatic energy storage elements, alternately charged positive and negative, that can be switched to produce a constant amplitude oscillatory waveform in the time domain that mimics the spatially stored energy. The oscillatory frequency of this wave is determined by the energy storage elements which can be made up of discrete components or alternately made from transmission line segments.

In this paper, we will review the state of the art in FWG technology, contrasting various techniques and range of frequencies attainable. In our laboratory, we have investigated a unique topology that reduces the number of switch elements to a single switch. In this paper we will present results for multi-cycle laboratory scale single-switch FWG RF sources for frequencies as high as 500 MHz. Scaling relations and designs for higher frequency and power will also be presented and discussed within the context of switch requirements and matching to radiating elements.

I. INTRODUCTION

There are numerous techniques for producing high Radio Frequency (RF) pulses at peak power levels greater than 100 MW. For frequencies below 500 MHz, Vector Inversion Generators configured as an oscillator, oscillators based on quarter wave transmission lines, and "lumped element" L-C oscillators are standard techniques typically used. The frequency of oscillation for such devices is inversely proportional to the square root of the product of the capacitance, C, and the inductance, L. For frequencies above 500 MHz, both the capacitance and inductance required for discrete LC oscillators become so small that stray effects tend to dominate and limit the frequency attainable. In the microwave region of the spectrum, devices such as Vircators, Backward Wave Oscillators, Relativistic Magnetrons, etc. are used. These microwave devices are usually large, and have limited efficiency, making it problematic to deploy in small portable payload spaces. In general, the wave packet generated by these techniques consists of a decaying sinusoid of a few cycles with only one or two of the cycles having high peak power. Further, the limited number of cycles and the use of spark switches tend to produce wide bandwidth making it difficult to accurately match the generator output to a radiating structure.

II. FROZEN WAVE GENERATOR

An alternate technique, the "frozen wave" generator" investigated for many years, can cover the range from low frequency to terahertz frequencies [1-4], producing a constant amplitude wave packet. The technique consists of segments of transmission line, alternately charged, with two segments constituting a single cycle. The length of each segment is one-half of a wavelength of the desired radiation. If perfect, the output from the device is a "square-top, equal-amplitude, multi-cycle waveform" with the number of cycles determined by the number of transmission line segments. The primary drawback to this technique in most embodiments is the need for a separate switch between each pair of segments. A schematic of a Frozen Wave Generator (FWG) is shown in Fig. 1.

* Work supported by the US ARMY SMDC, Contract # W9113M-12-C-0047
ξ email: sbest@radiancetech.com, frose@radiancetech.com, zshotts@radiancetech.com
Ψ email: mark.s.rader2.civ@mail.mil, larry.l.altgilbers.civ@mail.mil

Report Documentation Page

Form Approved
OMB No. 0704-0188

1. REPORT DATE	2. REPORT TYPE	3. DATES COVERED
JUN 2013	**N/A**	**-**

4. TITLE AND SUBTITLE	5a. CONTRACT NUMBER
Frozen Wave Generator Technology As A Source Of Constant Amplitude High Power High Frequency Radio Frequency Pulses	5b. GRANT NUMBER
	5c. PROGRAM ELEMENT NUMBER
6. AUTHOR(S)	5d. PROJECT NUMBER
	5e. TASK NUMBER
	5f. WORK UNIT NUMBER
7. PERFORMING ORGANIZATION NAME(S) AND ADDRESS(ES) **Radiance Technologies, Inc., 1490 Pumphrey Ave Auburn, Alabama, U.S.A.**	8. PERFORMING ORGANIZATION REPORT NUMBER
9. SPONSORING/MONITORING AGENCY NAME(S) AND ADDRESS(ES)	10. SPONSOR/MONITOR'S ACRONYM(S)
	11. SPONSOR/MONITOR'S REPORT NUMBER(S)

12. DISTRIBUTION/AVAILABILITY STATEMENT
Approved for public release, distribution unlimited

13. SUPPLEMENTARY NOTES
See also ADM002371. 2013 IEEE Pulsed Power Conference, Digest of Technical Papers 1976-2013, and Abstracts of the 2013 IEEE International Conference on Plasma Science. IEEE International Pulsed Power Conference (19th). Held in San Francisco, CA on 16-21 June 2013., The original document contains color images.

14. ABSTRACT
A Frozen Wave Generator as a source of RF energy consists of an ensemble of electrostatic energy storage elements, alternately charged positive and negative, that can be switched to produce a constant amplitude oscillatory waveform in the time domain that mimics the spatially stored energy. The oscillatory frequency of this wave is determined by the energy storage elements which can be made up of discrete components or alternately made from transmission line segments. In this paper, we will review the state of the art in FWG technology, contrasting various techniques and range of frequencies attainable. In our laboratory, we have investigated a unique topology that reduces the number of switch elements to a single switch. In this paper we will present results for multi-cycle laboratory scale single-switch FWG RF sources for frequencies as high as 500 MHz. Scaling relations and designs for higher frequency and power will also be presented and discussed within the context of switch requirements and matching to radiating elements.

15. SUBJECT TERMS

16. SECURITY CLASSIFICATION OF:			17. LIMITATION OF ABSTRACT	18. NUMBER OF PAGES	19a. NAME OF RESPONSIBLE PERSON
a. REPORT	b. ABSTRACT	c. THIS PAGE			
unclassified	**unclassified**	**unclassified**	**SAR**	**6**	

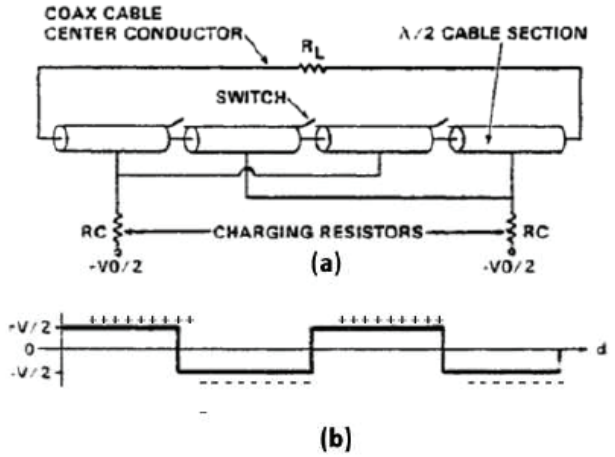

Figure 1. Two cycle frozen wave generator illustration. (a) Physical layout showing coaxial elements. (b) Static potential distribution showing polarity of each element in (a). (Reproduced from Forcier, et al., [5])

Referring to Fig. 1, the FWG consists of a linear, multi-switch ensemble of transmission line segments with alternate segments charged to opposite polarity. In this arrangement, energy from a power supply is statically stored in alternately charged sections of transmission line with constant characteristic impedance Zo. By simultaneously closing all of the switches in the ensemble, the spatially stored static electric charge distribution is converted to two dynamic waves moving through the line segments, in opposite directions, to the load R_L. The frequency of the resultant wave packet is determined by the length of each transmission line segment which for constant frequency requires each segment to be λ/2 in length. Figure 1 illustrates a two cycle device although many cycles can be produced by simply adding more line segments. Note that now all of the cycles in the wave packet are constant amplitude and for an ideal case would be "square-top." Dispersion and discontinuities represented by the switches tends to round the cycles especially at high frequencies. High frequency FWG RF sources based on the Fig. 1 schematic require;

- Sub-nanosecond switch synchronization
- External switch trigger generator
- Low loss switches
- Sub-nanosecond switch impedance collapse
- At least one switch per RF cycle.

The FWG devices described in References [1-4] use solid state switching with laser triggering which make it somewhat problematic to make a highly compact efficient source. Further, solid state switches have moderately high on-state resistance making the FWG less efficient as much of the energy is absorbed in the switch itself. This is especially important at high frequency where each line segment stores minimal energy.

In the FWG topology shown in Fig. 1, note that the ends of each individual transmission line segment are at the same potential. This fact allows the FWG to be arranged in a different 'folded' configuration which requires only one switch as shown in Fig. 2.

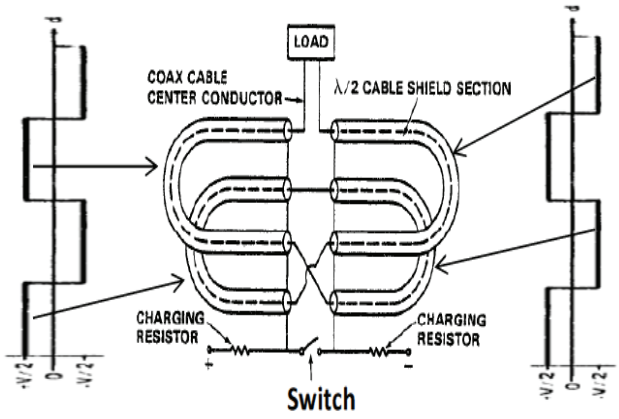

Figure 2. Folded frozen wave structure exactly equivalent in spatially stored charge as that shown in Fig. 1. (Reproduced from Forcier, et al., [5])

This 'folded' topology was first investigated by Forcier, Rose, Rhinehart, and Gripshover[5] for frequencies as high as 800 MHz. In this paper, we have extended the work in [5] using new materials and switch technology over a comparable frequency range and with as many as 10 constant amplitude cycles. Note that the center conductor of the coaxial transmission line is still continuous throughout the cable sections. In this configuration, the static or frozen wave is stored in the cable sections just as in Fig. l(b). When the switch is closed, the exact same process as described for the linear configuration is initiated with replicas of the frozen wave again traveling in both directions to the load – now all wave segments flow through one switch sequentially. More importantly, the switch impedance collapse loss occurs only one time and tends to affect only the first half cycle to transit the switch. As shown in Fig. 2, the frozen wave generator is a continuous length of the cable with a single discontinuity caused by the agglomeration of the outer braids of each section of line on opposite ends of the switch.

III. EXPERIMENTAL RESULTS

Initial experiments concentrated on reproducing some of the results from [5]. The first device consisted of a simple 1-cycle (2-segment) FWG constructed from RG-58/U coaxial cable as shown in Fig. 3. The two sides of the FWG were switched together with a modified "stab switch" which produced acceptable results. The observed waveforms, ideally flat-top, show fine structure due to non-ideal switching and load impedance conditions. The

frequency of operation is roughly 30 MHz and agrees well with the segment line element whose length is cut to one half wavelength. From these tests, we were comfortable that we could accurately diagnose and characterize FWG experimental prototypes.

(a.)

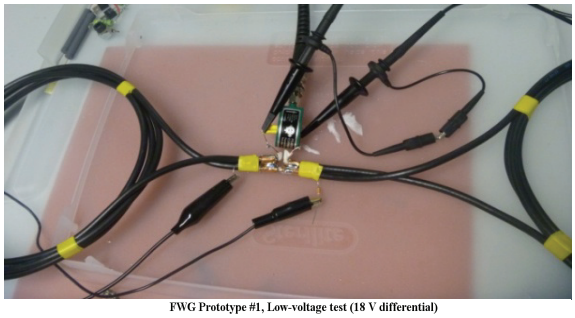

(b.)

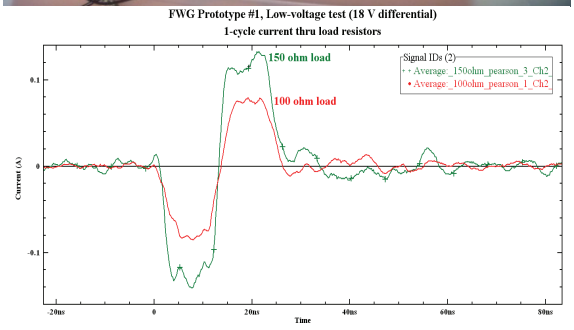

Figure 3. First single cycle FWG test article. (a) Assembled unit showing general arrangement of segments. (b) Waveform for two resistive loads. Frequency is approximately 30 MHz.

Several FWG prototypes were built with this technique. Fig. 4 shows a device similar in construction to that shown in Fig. 3 that operated at 550 MHz. Note that there is "late time" ringing due to mismatch between the line segment impedance and the load. Simple stab switching produced wide variability in the amplitude, impedance mismatch and noise in the diagnostics.

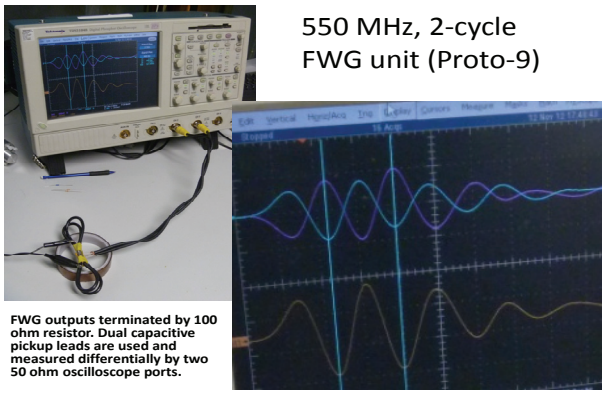

Figure 4. Test setup with Averaged waveform approx. 550 MHz measured differentially. Top trace shows individual waves propagating in opposite directions within the FWG. Bottom trace is the differential sum.

Based on these initial tests, a FWG switch manifold testbed was built which allowed up to 4 RF cycles in a geometry that insured repeatable switching conditions and allowed switching to be accomplished by "overvolting" in a SF_6 or H_2 environment at operating voltages in excess of 2 kV. This testbed structure was tested with many different configurations of line segments to support various frequencies, number of cycles, types of coaxial cable, and different load termination schemes.

Signal diagnostics in the FWG structure presents challenges at very high frequencies which in some cases were addressed through the use of attaching radiative antenna loads in lieu of simple resistive loads. In some cases we attached a simple dipole antenna to a 4-cycle FWG RF unit assembled using this switching manifold assembly and operated it at voltages as high as 2.6 kV in SF_6.

We received the RF radiated signal waveform using a Vivaldi Antenna that had been calibrated for use in this frequency band. Fig. 5 shows the received waveform. Note that both the beginning and end of the wave packet is "rounded' due to the antenna transfer functions for both transmit and receive. Note also, reflections of the wave packet from metallic objects in the vicinity of the receive antenna. Experiments were conducted in a high bay area of the lab.

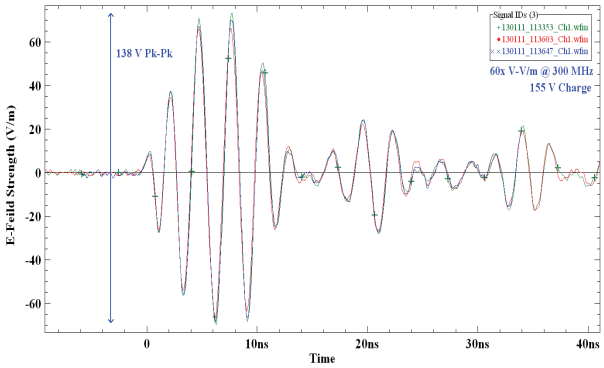

Figure 5. E-field Strengths (@ 1m range) from 300 MHz FWG using FWG integral-dipole antenna.

By varying the switch gas conditions, we were able to determine E-field strength scaling for the FWG device as a function of FWG charge voltage. Figure 6 shows the peak E field strength as a function of FWG charge voltage from the 4-cycle FWG shown in Fig 4 as measured using the Vivaldi antenna at a 1m range. Note that in the RF antenna radiated far field, the E-field scales with charge voltage at a constant value of range as, E = KV/R where K is a constant for a given antenna configuration. Note from Fig. 6 that, as expected, the functional dependence of measured E-field strength as a function of charge voltage is linear.

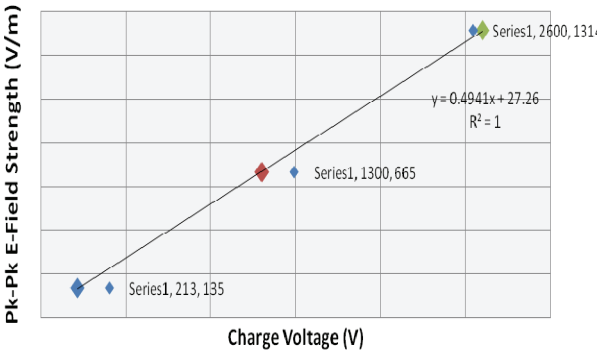

Figure 6. E-field Strength (1m range) as a function of FWG Charge Voltage of the 4-cycle FWG shown (Fig 4).

IV. MODELING AND SIMULATION

In our experiments, it was obvious that the switch parameters would affect the FWG and would be critical to designs as the frequency of the FWG increased. To examine the effect of switch parameters, we simulated the FWG using a ladder LC approximation to the individual line segments. Spice models were constructed and simulations run using LTspice® IV. Figure 7 shows an example Spice model for a 10-cycle FWG. Different LC ladder networks were designed as sub-circuit components and used within the upper level FWG models.

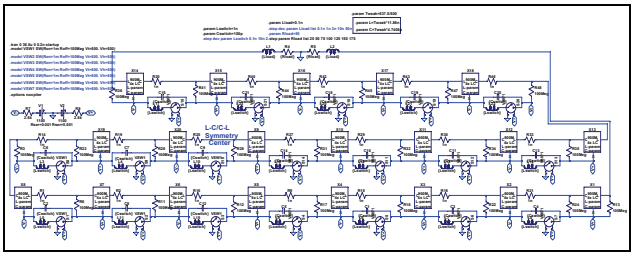

Figure 7. Spice model of a 10-cycle FWG.

Switch capacitance and inductance were based on values achieved in other work and can be attained in the switch manifold geometry. In the Spice model, the switch was assumed to consist of a "perfect" closure mechanism with RLC values: low series resistance, inductance L representing the spark and electrode contributions, and a capacitance C in parallel also representing the switch housing contributions. Switching closing-time and opening-time (recovery) period could also be specified. In that configuration, the switch impedance can be calculated as $(L/C)^{1/2}$ and can be used as a "figure of merit" for determining the effect of the switch on the frequency of the FWG. To "benchmark" the model, we simulated 150, 300, 500, and 600 MHz 4-cycle FWGs for which we have experimental data. Figure 8(a) shows the experimental trace with the comparable Spice simulation in Fig. 8(b). Note the waveforms are similarities.

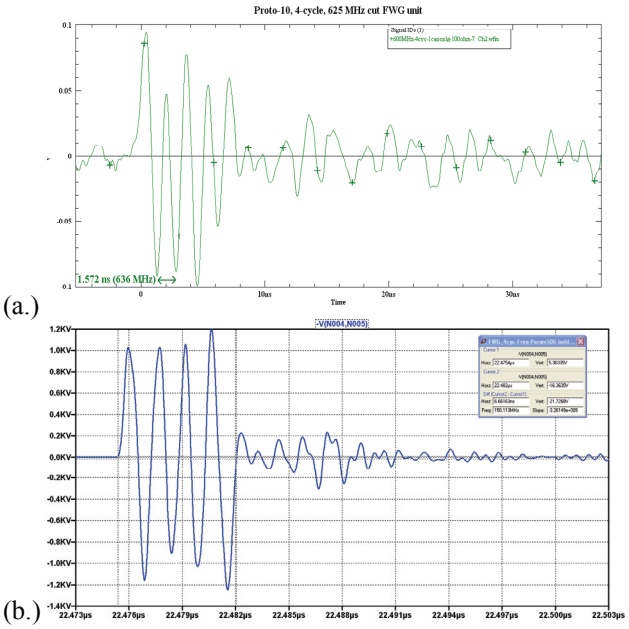

Figure 8. Benchmark experimental results; (a) Measured waveform for a 4-cycle nominal 600 MHz FWG. (b) Spice simulation of a 4-cycle 600 MHz FWG.

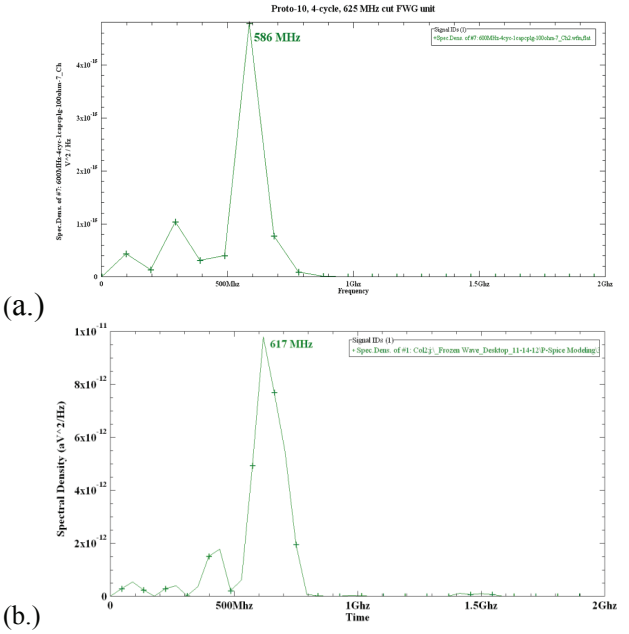

Figure 9. Fourier transforms of Fig. 8 (a.) Experimental waveform results and, (b.) Simulated 600 MHz FWG generator results.

Figure 9 contains Fast Fourier transforms for the waveform and simulation data shown in Fig. 8. Note that the modeled and measured spectral distributions are highly similar but differ in frequency by a few percent.

This is due in part to the fact that we may not have accurate switch parameters for the model.

Based on successful benchmarking of the model, we used the Spice model to investigate the effect of switch parameters on frequency for a 4-cycle 900 MHz FWG. Figure 10 shows the results of simulation of a 900 MHz, 4-cycle FWG where L is held constant and C is varied over an order of magnitude.

Note that the switch manifold capacitance lowers the design frequency and will be a design parameter that must be accounted for in specific FWG device designs. Figure 11 shows the results of a series of simulations where the switch impedance is varied by changing the switch inductance for fixed values of capacitance.

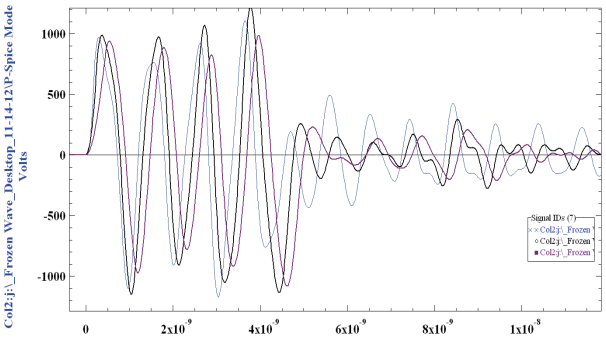

Figure 10. Effect of switch capacitance on 4-cycle nominal 900 MHz FWG. Switch inductance assumed to be 1 nH. (Horizontal time axis units: seconds.)

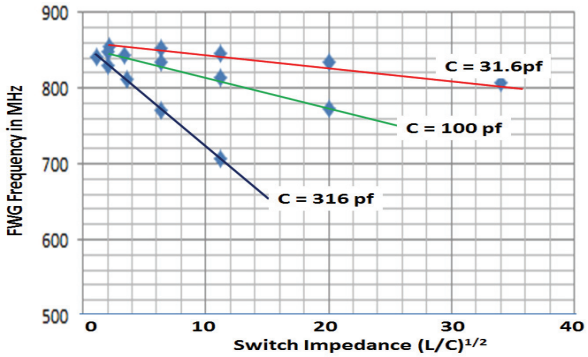

Figure 11. Effect of spark switch impedance on the modeled 900 MHz FWG. Impedance changes were made for specific fixed capacitance values by varying the switch inductance.

From Fig. 11, it is obvious that a small value of the switch impedance as defined above is necessary to minimize the effect of the switch on FWG design frequency. From these data, we are confident that FWG devices can be built at frequencies approaching 1 GHz.

Figure 12 shows clearly the differences between typical high power RF impulsive sources based on LC oscillators and frozen wave generators. The design of the FWG allows the RF loads to continue to be energized by the n-cycle wave-train created by the FWG (Fig. 12a). The impulsive RF source signal however is enveloped due to initial charge-up and subsequent decay as the impulse energy is radiated or dissipated (Fig. 12b).

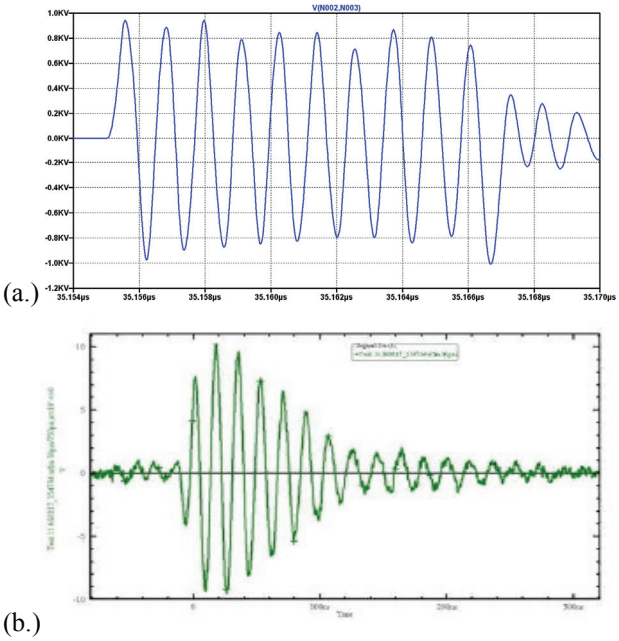

Figure 12. Contrast between waveforms for impulse transmitters. (a) Simulation of 10 cycle FWG. (b) Radiated waveform from a 60 MHz LC spark switched oscillator.

V. SCALING TO HIGHER POWER AND HIGH FREQUENCY

Figure 6 clearly shows radiated E-field scaling with increased operating voltage for voltage greater than 2 kV. Since the simple physics of electromagnetic radiation phenomena show that for a fixed distance from the transmitter, the measured E-field scales with voltage applied to the terminals of the antenna, our experimental devices are in fact oscillators and not spurious noise generated by the spark switch. Further as shown above, the measured waveforms and that obtained by modeling with Spice are similar enough to give high confidence that scaling to high voltages is both practical and easily implementable over a wide frequency range.

The FWG switch manifold assemblies have been manufactured to spark switch inductance and capacitance parameters that have been achieved in other spark switches that functioned at high repetition rates. Using these switch parameters, the Spice modeling shows that scaling to higher power levels and higher operating voltages are possible with minimal degradation of the wavepacket. Since the characteristic impedance of the transmission line segment impedance Zs governs the load impedance Z_L, then $Z_L = 2Zs$. For ease of matching to a dipole-type antenna load with characteristic impedance of ~73 ohms, the transmission line segment characteristic

impedance Zs should be on the order of 35-37 ohms. High voltage coaxial cable is available commercially for voltages as high as 40 kV DC and with characteristic impedance ranging from 31 ohms to 50 ohms. Insertion of these cables into the switch manifold and configured for higher voltages should allow multi-cycle devices with frequencies as high as 1 GHz to be fabricated and tested.

Extrapolating the data in Fig. 7 to an operating voltage of 30 kV would give an E-field strength at one meter of approximately 15 kV/m. Adding a simple 3 element Yagi-Uda antenna with a gain of 7 dB, the E-field strength as calculated from Eq. 1,

$$E = \frac{\sqrt{30 P_T G_T}}{r} \text{ V/m} \qquad (1)$$

is about 50 kV/m at one meter range. P_T is the power delivered to the antenna, G_T is the transmitter gain in dB and r is the distance from the transmitter to the point where the measurement is made. Note that at 500 MHz (λ=0.6 m), one meter range is in the far field.

VI. CONCLUSIONS AND DISCUSSION

For a conventional spark-switched LC oscillator, the wavepacket consists of an exponentially decaying sinusoid with the number of cycles dependent on losses and how well the oscillator is matched to a load (antenna). As energy is radiated from the system or absorbed internally, the spark switch impedance begins to recover resulting in decreased frequency in the late time. This spreading of the frequency increases the bandwidth of the wavepacket and decreases the efficiency of the coupling between the oscillator and the antenna system.

By contrast, the FWG oscillator produces a "constant amplitude" wavepacket with minimal frequency spreading since the switch sees a constant amplitude wave. We do however see, both in the modeling and experimentally, that the first half cycle and the last half cycle of the wave is spread and is due to the fact that energy from the line segments is transferred to the switch inductance as the switch closes with a characteristic time constant that depends on the switch inductance. Similarly, after the last line segment is absorbed in the load, the energy still in the switch inductance can distort the last half cycle in the packet as it too is absorbed at the load. Note, however that the switch capacitance is charged from the energy source prior to switch closure and is at the same potential as the line segments.

Although we have only investigated this technique experimentally to approximately 600 MHz, the results of modeling and switch parameters that we know are achievable, give high confidence that frequencies approaching 1 GHz are achievable in multi-cycle FWG RF sources.

VII. REFERENCES

[1] "High Power Microwave Generation Using Optically Activated Semiconductor Switches," W. C. Nunnaly, IEEE Tran. Electron Devices. Vol. ED-17, No. 12. Dec. 1990

[2] "Compact Optically Triggered Microwave Pulse Generation," M. L. Riaziat and C. K. Nishimoto, Microwave and Optical Technology Letters, Vol. 5, No. 5, May 1992

[3] "Frozen wave generation of bandwidth-tunable two-cycle THz radiation," J. F. Holzman, F. E. Vermeulen, and A. Y. Elezzabi, J. Opt. Soc. Am. B, Vol. 17, No. 8 / August 2000

[4] "An Ultra Wideband Impulse Optoelectronic Radar," M. Lalande, et. Al. Progress In Electromagnetics Research B, Vol. 11, 205–222, 2009

[5] "Frozen Wave Generators: Theory and Application," M. L. Forcier, M. F. Rose, L. Rhinehart, R. Gripshover, Proc. 1st IEEE International Pulsed Power Conference, PP 221-225, Lubbock Texas, 1979.